THE UNIVERSITY OF MICHIGAN

COLLEGE OF ENGINEERING
Department of Electrical Engineering
Space Physics Research Laboratory

Scientific Report No. GS-3

THEORY OF CURRENT COLLECTION OF MOVING CYLINDRICAL PROBES

Prepared on behalf of the project by:

Madhoo Kanal

ORA Projects 03484 and 04304

under contract with:

NATIONAL AERONAUTICS AND SPACE ADMINISTRATION
CONTRACT NO. NASr-15
WASHINGTON, D.C.

and

GEOPHYSICS RESEARCH DIRECTORATE
AIR FORCE CAMBRIDGE RESEARCH LABORATORIES
OFFICE OF AEROSPACE RESEARCH
UNITED STATES AIR FORCE
CONTRACT NO. AF 19(604)-6124
BEDFORD, MASSACHUSETTS

administered through:

OFFICE OF RESEARCH ADMINISTRATION ANN ARBOR

November, 1962

TABLE OF CONTENTS

LIST OF FIGURES

LIST OF SYMBOLS

W	drift velocity of the probe
C_m	most probable velocity of a particle ($= \sqrt{2kT/m}$)
λ	$= W/C_m$
Θ	angle between the drift velocity W and axis of the cylinder
κ	$= \lambda \sin \Theta$
u'_x, u'_y, u'_z	components of a particle velocity along x', y', z' axes, respectively, fixed in space
u_x, u_y, u_z	relative components of a particle velocity along x, y, z axes, respectively, when the probe is moving
T	temperature (°K)
N	number of particles per cubic meters
e	unit charge, 1.602×10^{-19} coulombs
m	mass of a particle in kgm
k	Boltzmann's constant 1.3803×10^{-23} joule/°K
V	potential of the collector with respect to the plasma
$\overline{V}$	normalized potential = eV/kT
I	current to the collector
I_n	normalized current = $I/\sqrt{kT/2m\pi}\ NeA_c$
A_c	area of the collector
a	radius of the sheath
r	radius of the collector
γ_o	symbol for $\sqrt{r^2/(a^2-r^2)}$

L	length of the collector
δV	voltage applied between the cylindrical collector and the reference
ρ	closest point of approach of particle to collector

ABSTRACT

The theory of current collection of a moving cylindrical probe is investigated. Volt-ampere relations are derived for two distinct cases: (i) The general-ion current for accelerating collector potential and its special cases, including general-ion current to the stationary probe, orbital-motion-limited current to the moving and the stationary probes, and sheath-area-limited current to the moving and the stationary probes; and (ii) The general-electron current for retarding collector potential and its special cases, including general-electron current to the stationary probe and random-electron current to the moving and the stationary probe. Orientation of the cylinder with respect to the drift velocity vector is taken into account. Volt-ampere characteristics are included for illustrating the functional behavior of the current relations.

1. INTRODUCTION

As the study of the ionosphere has progressed through the years, refinements made in vertical sounding equipment and analysis techniques have exposed the more complex nature of the ionosphere and thus demonstrated the necessity for more direct measurements. Such measurements became possible after World War II with the advent of sounding rockets. The University of Michigan investigators suggested the use of Langmuir probes for such measurements, and in 1946 and 1947 three successful V-2 flights carried such probes in their payload. However, the design and location of the probes were dictated by the other instruments used, and consequently there was much uncertainty in the data. This uncertainty was attributed to:

(a) failure of the probes to approximate any ideal geometry;

(b) overlapping of the sheath of the electrode with that of the rocket;

(c) perturbations in the density distribution of the particles caused by the high velocity of the rockets; and

(d) contamination of the region around the rocket by rocket gases.

In view of the uncertain results obtained in these earlier attempts to use rocket-mounted probes, complete ejection of the probe from the rocket was considered necessary to reduce the ambiguities substantially. Two different probe configurations answering these requirements have been developed: a Dumbbell-shaped bipolar probe,[1,2] which in more recent flights was combined with cylindrical Langmuir probes; and a combination spherical ion trap and cylindrical Langmuir probe.[3] In recent years, with the advent of multi-

experimental satellites, single cylindrical Langmuir probe experiments are also gaining popularity. In all these experiments, as is normal for rocket-borne probes, the rocket velocity exceeds the characteristic velocity of the ions for much of the flight. Thus the data obtained indicate strong effects of the probe velocity on the ion current collected by the device, thereby drawing attention to the need for a theoretical development which would permit the volt-ampere relation to be predicted as a function of the probe velocity, and would thus aid in the reduction of the data from the flights.

Mott-Smith and Langmuir[4] published their classic paper on probe theory in 1926, in which they derived the volt-ampere characteristics for spherical, cylindrical, and planar probe geometries. In their treatment they assumed a stationary plasma having a Maxwellian distribution, and did not consider the effect of drift velocities except for the case of electron current collection by a thin cylindrical probe whose axis was at a right angle to the drift velocity. It is, therefore, necessary to investigate the general theory of current collection, particularly in regard to high probe velocities and collectors of various sizes. In this report the aim is fulfilled for cylindrical collectors only. The problem of moving spherical collectors was treated by the author in an earlier report.[5]

2. THEORY OF CURRENT COLLECTION OF MOVING CYLINDRICAL PROBES

2.1 GENERAL CONSIDERATIONS

When a cylindrical electrode is immersed in a plasma consisting of positive ions and electrons having Maxwellian velocity distribution, the resulting collisions of the charged particles with the probe cause it to assume an equilibrium potential with respect to the plasma such that the net current to the collector is zero. If the medium is in thermal equilibrium, which means that the mean energies of the ions and electrons are equal, then the magnitude of the equilibrium potential is mainly determined by the square root of the ion-to-electron mass ratio and the resulting polarity of the probe is negative. The collector potential causes a region of positive charge to build up about the probe in which electrons are repelled and positive ions are attracted. Such a region is commonly called a positive-ion-sheath. The boundary of the sheath is defined as that distance beyond which the charged particles experience negligible force due to the probe potential.

Since the primary purpose of this study is to evaluate the effects of the sheath upon the current collection when the probe is moving, some assumption in regard to the sheath configuration is necessary. Although the cylindrical shape of the sheath will not be maintained at high probe velocities, no sufficiently precise model is available which will justify empirically or theoretically any other shape. Therefore, as a first-order approximation a cylindrical sheath is assumed.

2.1.1 Ion Current

In evaluating the effects of the sheath on the ion current collection, three distinct cases are encountered throughout the range of possible values of T/Nr^2, where T is the mean temperature, N is the particle number density, and r is the radius of the collector.

(a) When $T/Nr^2 \lesssim 5 \times 10^{-6}$, the ion current collected by the electrode is termed "sheath-area-limited." In other words, all the ions that enter the sheath from the ambient plasma reach the collector. Mathematically this condition of collection is achieved by letting $a/r \to 1$, where a is the sheath radius.

(b) When $T/Nr^2 \gtrsim 10^{-3}$, the ion current collected is termed "orbital-motion-limited." Ion collection under this condition is dependent only upon the net voltage across the sheath and is practically independent[4] of the sheath radius. Mathematically this may be expressed by letting $a/r \to \infty$.

(c) When $5 \times 10^{-6} < T/Nr^2 < 10^{-3}$, the ion current collected is termed "intermediate." In this case the probability of collecting an ion is dictated by both the sheath radius and the net voltage across the sheath.

As seen from the foregoing discussion the sheath-area-limited and the orbital-motion-limited conditions of ion collection constitute the asymptotic extremes of the general case. It should also be noted that the ranges of T/Nr^2, where each class of ion collection is implied, are subject to some change when the probe is moving with high drift velocity. However, for a

stationary probe these figures are generally accurate.[1]

2.1.2 Electron Current

In the case of electron current collection which is independent of the sheath radius,[6] essentially two distinct cases are encountered throughout the range of possible negative collector potential.

(a) When the collector potential, V, is near zero with respect to the plasma, the electron current collected under this state is termed "random."

(b) When a finite negative collector potential exists with respect to the plasma, the probability of an electron's reaching the collector is dictated by V, and the current collected by the electrode is termed "general."

Since in most ionosphere experiments the probe velocities never even come close to the mean velocity of the electrons, the probe motion has little effect on the electron current collection and can be neglected. However, the probe motion must be taken into account in the case of negative ion collection because of the heavier mass and hence the low mean velocity. For this reason the theory developed here takes account of probe velocity for both the ion and electron collection cases, but in the discussion of volt-ampere characteristics (Section 3) the velocity effect on electron current is neglected.

2.1.3 Sign Convention

In deriving the current functions for ions and electrons when the collector potential is either accelerating or retarding for any of the particles,

it is expedient to refer to the actual polarities of the collector and of the particles. Therefore in considering the trajectories of the charged particles in the sheath the polarities of both the particles and the collector are retained and a proper selection of the signs is made in setting up the current equations.

2.2 TRAJECTORY OF A CHARGED PARTICLE IN THE SHEATH

Let "a" be the radius of the sheath concentric with the cylindrical collector of radius "r" and length "L" ($L \gg r$). Consider the moving probe such that its axis is perpendicular to the plane of the paper, as shown in Fig. 1. Let p and u_x be the relative tangential and normal velocity components respectively of a charged particle ($\pm e$), at the sheath edge in a plane normal to the axis of the probe. Let p_c and u_c be the corresponding quantities near the collector surface. Then from the laws of conservation of energy and angular momentum we have:

$$p^2 + u_x^2 = p_c^2 + u_c^2 + \frac{2(\pm e)(\pm V)}{m} \tag{1}$$

$$ap = \rho p_c \tag{2}$$

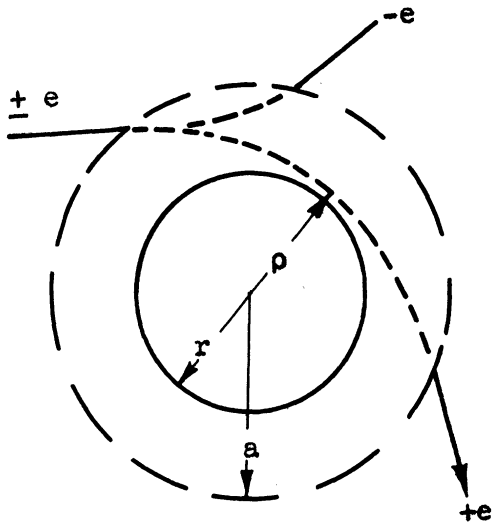

Fig. 1. Trajectory of a charged particle in the sheath.

where e is the unit charge, V is the collector potential with respect to the plasma, and ρ is the closest point of approach of the particle to the collector. In Eq. (1) when we consider a positive ion (+e) encountering a negative collector potential (-V), the product (+e)(-V)—which represents gain in energy in the sheath--becomes negative, and in accordance with the physical situation that product must be subtracted from the right-hand side of Eq. (1). In this way we can consider other cases of particle-field interaction and select the proper signs when required. Further consideration of Eqs. (1) and (2) suggests that only those particles will reach the collector for which $u_X > 0$, $u_c^2 \geq 0$. If we substitute Eq. (2) in Eq. (1) for p_c, put $u_c = 0$, $p = p_1$, $\rho = r$, and rearrange the terms we obtain

$$p_1^2 = \frac{r^2}{a^2-r^2}\left[u_X^2 - \frac{2(\pm e)(\pm V)}{m}\right] \qquad (3)$$

Equation (3) thus describes the condition necessary for the collection of a charged particle for a given collector potential and dimension.

Next we will consider the Maxwellian velocity distribution of the particles with respect to a coordinate system which is fixed in the plasma and then view the same distribution function from a coordinate system which is fixed on the moving probe. The latter we will term "the superimposed Maxwellian."

2.3 SUPERIMPOSED MAXWELLIAN DISTRIBUTION

Consider an oblique view of the cylindrical sheath as shown in Fig. 2. Let x', y', z' be a set of three orthogonal axes fixed in space representing in direction and magnitude the three components u_X', u_Y', u_Z' of the particle

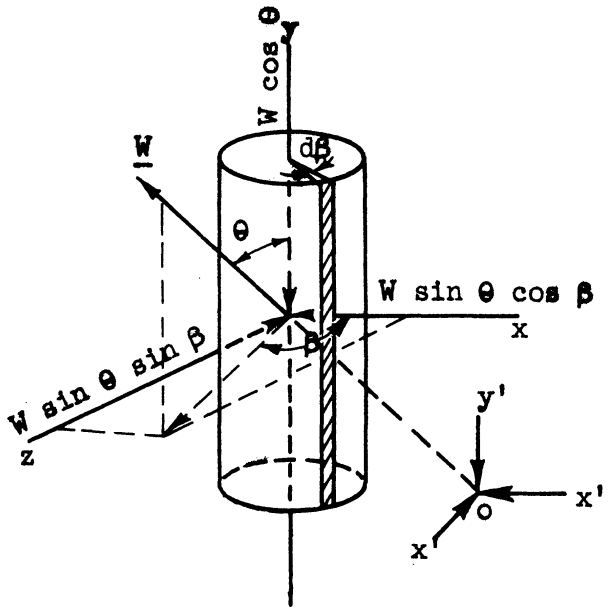

Fig. 2. Velocity space coordinates at the sheath surface.

velocity, respectively. Let x, y, z be another set of three orthogonal axes, parallel to the first one, fixed on the moving probe, and representing in direction and magnitude the three relative components u_x, u_y, u_z of the particle velocity, respectively. Choose y-axis along the axis of the cylinder as shown. If W is the probe velocity and θ the angle between $\underline{W}$ vector and y-axis, then the components of $\underline{W}$ superimposed on u'_x, u'_y, u'_z are W sin θ cos β, W cos θ, W sin θ sin β, respectively. In other words,

$$\begin{aligned} u_x &= u'_x + W \sin\theta \cos\beta \\ u_y &= u'_y + W \cos\theta \\ u_z &= u'_z + W \sin\theta \sin\beta \end{aligned} \tag{4}$$

where β is the azimuth angle of $\underline{W}$ with respect to x-axis.

Let N be the number density of one kind of particle in the plasma, T the mean temperature, and m its mass; then the Maxwellian velocity distribution

of the particles with respect to the stationary coordinate system is

$$f(u'_x,u'_y,u'_z)\,du'_x du'_y du'_z = \frac{N}{(\pi C_m^2)^{3/2}} \exp\left[-\frac{1}{C_m^2}\left(u_x'^2 + u_y'^2 + u_z'^2\right)\right] du'_x du'_y du'_z \qquad (5)$$

where C_m is the most probable velocity of the particles defined as $C_m = \sqrt{2kT/m}$, k being the Boltzmann's constant. With respect to the moving system the distribution function (5) is modified in a way determined by the linear transformations of the velocity components given in Eqs. (4). Thus for the moving system the new distribution function is

$$F(u_x,u_y,u_z,\beta)\,du_x du_y du_z = \frac{N}{(\pi C_m^2)^{3/2}} \exp\left[-\frac{1}{C_m^2}\left\{(u_x - W\sin\theta\cos\beta)^2 + (u_y - W\cos\theta)^2 + (u_z - W\sin\theta\sin\beta)^2\right\}\right] du_x du_y du_z \qquad (6)$$

which represents the superimposed Maxwellian velocity distribution.

2.4 GENERAL-ION-CURRENT FUNCTION FOR AN ACCELERATING POTENTIAL (-V)

In Fig. 2 consider an infinitesimal strip of area (L a dβ) on the sheath surface. The number of ions with velocity ranges between u_x and u_x+du_x, u_y and u_y+du_y, and u_z and u_z+du_z that are expected to cross the infinitesimal area per unit time is given by

$$Lau_x F(u_x,u_y,u_z,\beta)\,du_x du_y du_z d\beta \qquad (7)$$

On multiplying Eq. (7) with the ionic charge and integrating between the proper limits we obtain the following equation for the ion current collected by the moving probe.

$$I_i = Lae \int_{\beta=0}^{2\pi}\int_{u_x=0}^{\infty}\int_{u_y=-\infty}^{\infty}\int_{u_z=-p_1}^{p_1} u_x\, F(u_x,u_y,u_z,\beta)\,du_x du_y du_z d\beta \qquad (8)$$

In Eq. (8) the limits of u_y range from $-\infty$ to ∞ because we have assumed that $L \gg r$. The limits of u_z are from $-p_1$ to p_1 because if in a plane normal to the cylinder u_x is the radial component at the sheath surface, then u_z represents the tangential component for which the trajectory (3) determines the values of $\pm p_1$.

It is trivial to integrate Eq. (8) for β and u_y. Integration with respect to u_z is carried out in Appendix A. The final result, in terms of the sum of two single integrals, is given in Eq. (9).

$$I_i = \sqrt{\frac{kT}{2m\pi}}\, NeA_c \frac{4}{\sqrt{\pi}}\, e^{-\kappa^2} \left[\int_{\gamma_o\sqrt{\nabla}}^{\infty} s(s^2+\nabla)^{1/2} e^{-s^2} I_o(2\kappa s)\, ds \right.$$

$$\left. + \sqrt{\frac{1+\gamma_o^2}{\gamma_o^2}} \int_0^{\gamma_o\sqrt{\nabla}} s^2\, e^{-s^2} I_o(2\kappa s)\, ds \right] \qquad (9)$$

where

$$\kappa = \lambda \sin\theta$$

$$\lambda = W/C_m = W/\sqrt{2kT/m}$$

$$\gamma_o = \sqrt{r^2/(a^2-r^2)}$$

$$\nabla = eV/kT$$

$$A_c = 2\pi rL \text{ (area of the collector)}$$

and s is the new variable.

For obtaining numerical values it is expedient to perform numerical integration of (9). However, it is desirable to present the analytical solution for the sake of completeness. Appendix B contains the elementary steps involved in arriving at the solution of Eq. (9) given in Eq. (10).

$$I_i = \sqrt{\frac{kT}{2m\pi}}\, NeA_c \frac{2}{\sqrt{\pi}} e^{-\kappa^2} \left\{ e^{-V} \sum_{n=0}^{\infty} \frac{(\kappa\sqrt{V})^n}{n!} \Gamma\left[n + \frac{3}{2},\ V(1+\gamma_o^2)\right] J_n(2\kappa\sqrt{V}) \right.$$

$$\left. + \sqrt{\frac{1+\gamma_o^2}{\gamma_o^2}} \sum_{n=0}^{\infty} \frac{\kappa^{2n}}{(n!)^2} \gamma\left(n + \frac{3}{2},\ \gamma_o^2 V\right) \right\} \qquad (10)$$

where $\Gamma(\nu,x)$ and $\gamma(\nu,x)$ are the incomplete gamma functions bearing the following relationship

$$\Gamma(\nu,x) = \int_x^{\infty} e^{-t}\, t^{\nu-1}\, dt = \Gamma(\nu) - \gamma(\nu,x)$$

and $J_n(x)$ is the Bessel function of order n.

In order to visualize the effects of the sheath upon the current collection, let us define a normalized current, I_n, which is simply the collected current, I, divided by the current which would have resulted without the sheath. Mathematically

$$I_n = \frac{I}{\sqrt{\frac{kT}{2m\pi}}\, NeA_c} \qquad (11)$$

Thus, in the normalized form, the general-ion-current equation (10) becomes

$$I_{ni} = \frac{2}{\sqrt{\pi}} e^{-\kappa^2} \left\{ e^{-V} \sum_{n=0}^{\infty} \frac{(\kappa\sqrt{V})^n}{n!} \Gamma\left[n + \frac{3}{2},\ V(1+\gamma_o^2)\right] J_n(\kappa\sqrt{V}) \right.$$

$$\left. + \sqrt{\frac{1+\gamma_o^2}{\gamma_o^2}} \sum_{n=0}^{\infty} \frac{\kappa^{2n}}{(n!)^2} \gamma\left(n + \frac{3}{2},\ \gamma_o^2 V\right) \right\} \qquad (12)$$

When the probe velocity is small compared with the most probable velocity of the ions—in other words, when λ is small or when the probe is moving with its axis pointing in the direction of the velocity vector, $\Theta = 0$—then $\kappa = 0$.

Under these conditions it can be shown that Eq. (12) reduces to

$$I_{ni}\big|_{\kappa\to 0} = \sqrt{\frac{1+\gamma_o^2}{\gamma_o^2}}\,\mathrm{erf}(\gamma_o\sqrt{\nabla}) + e^{\nabla}\,\mathrm{erfc}\left[\sqrt{\nabla(1+\gamma_o^2)}\right] \qquad (13)$$

which, therefore, represents the general-ion-current function when $\kappa = 0$. In Eq. (13) error functions are defined as usual:

$$\mathrm{erf}(x) = \frac{2}{\sqrt{\pi}}\int_o^x e^{-t^2}\,dt$$

$$\mathrm{erfc}(x) = \frac{2}{\sqrt{\pi}}\int_x^\infty e^{-t^2}\,dt$$

Equation (13), which was previously derived by Langmuir[4] in 1926, has been used in various studies of plasmas involving space charge tubes as well as low speed probes in the ionosphere measurements of temperature and density. With modern high speed rockets, which during most of their trajectories exceed the most probable velocity of the ions, it has become necessary to take into account the probe motion. In such a case Eq. (12) must be used.

Because the cylindrical Langmuir probe is usually operated in the orbital-motion-limited mode, this particular case is examined in detail. As a special case of the general-ion-current function given in Eq. (12) we can deduce the orbital-motion-limited ion current function by letting $\gamma_o \to 0$, since $\gamma_o = \sqrt{r^2/(a^2-r^2)}$. However, it is much simpler to let $\gamma_o \to 0$ in Eq. (9), which is the general-ion-current function still in the integral form, than to take the limit of Eq. (10) as such. Similarily, in deducing the sheath-area-limited ion current function it is easier to let $\gamma_o \to \infty$ in Eq. (9) than in Eq. (12).

2.4.1 Orbital-Motion-Limited Ion Current Function

By letting $a/r \to \infty$ or, correspondingly, by letting $\gamma_o \to 0$ in Eq. (9), we obtain the ion current function which is independent of the sheath radius. It can be easily proven that when $\gamma_o \to 0$, Eq. (9) reduces to

$$I_{no} = I_i|_{\gamma_o \to 0} = \sqrt{\frac{kT}{2m\pi}}\, NeA_c \frac{4}{\sqrt{\pi}} e^{-\kappa^2} \int_o^\infty s(s^2+\bar{V})^{1/2} e^{-s^2} I_o(2\kappa s)\, ds \qquad (14)$$

Solution of the above integral is given in Appendix C. The final result in the normalized form is

$$I_{no} = e^{\bar{V}-\kappa^2} \sum_{n=0}^{\infty} \frac{(2n+1)!}{(n!)^2 2^{2n}} \left[\left(\frac{\kappa}{\sqrt{\bar{V}}}\right)^n J_n(2\kappa\sqrt{\bar{V}}) - (-1)^n \left(\frac{\sqrt{\bar{V}}}{\kappa}\right)^{n+\frac{3}{2}} J_{n+\frac{3}{2}}(2\kappa\sqrt{\bar{V}}) \right] \qquad (15a)$$

In a more sophisticated form Eq. (15a) may be written as

$$I_{no} = \frac{2}{\sqrt{\pi}} e^{\bar{V}-\kappa^2} \sum_{n=0}^{\infty} \frac{(\kappa/\sqrt{\bar{V}})^n}{n!} \Gamma(n+\tfrac{3}{2}, \bar{V}) J_n(2\kappa\sqrt{\bar{V}}) \qquad (15b)$$

where $J_n(x)$ and $J_{n+3/2}(x)$ represent the Bessel functions of index n and n + 3/2, respectively, and $\Gamma(n+\frac{3}{2}, \bar{V})$ is the incomplete gamma function.

For a stationary probe or when $\Theta = 0$, the current function (14) assumes a simpler form:

$$I_{no}|_{\kappa \to 0} = \frac{2}{\sqrt{\pi}} \sqrt{\bar{V}} + e^{\bar{V}} \operatorname{erfc}(\sqrt{\bar{V}}) \qquad (16)$$

For values of $V \geq 5$, Eq. (16) can be approximated by

$$I_{no}|_{\kappa \to 0} \cong \frac{2}{\sqrt{\pi}} \sqrt{1+\bar{V}} \qquad (17)$$

Equations (16) and (17) are well known and have been used extensively in laboratory plasma studies.[1,4] As mentioned above, however, in the study of the ionosphere by means of probes carried by sounding rockets or satellites, the probe motion makes it imperative to use Eq. (15a) or (15b).

2.4.2 Sheath-Area-Limited Ion Current Function

The sheath-area-limited condition is attained when all the ions that enter the sheath reach the collector. Mathematically, the functional representation of the current can be obtained by letting $a/r \to 1$ or $\gamma_o \to \infty$ in Eq. (9). The limit of Eq. (9) when $\gamma_o \to \infty$ yields

$$I_s = \sqrt{\frac{kT}{2m\pi}}\, NeA_c\, (a/r)\, \frac{4}{\sqrt{\pi}}\, e^{-\kappa^2} \int_o^\infty s^2\, e^{-s^2}\, I_o(2\kappa s)\, ds \qquad (18)$$

After solving the above integral, the normalized sheath-area-limited current is given by

$$I_{ns} = \frac{a}{r}\, e^{-\kappa^2} \left[(1+\kappa^2) I_o(\kappa^2/2) + \kappa^2 I_1(\kappa^2/2)\right] \qquad (19)$$

where $I_o(x)$ and $I_1(x)$ are the modified Bessel functions of the order of zero and one, respectively.

For stationary probe or when $\Theta = 0$, Eq. (19) reduces to

$$I_{ns}\big|_{\kappa \to 0} = \frac{a}{r} \qquad (20)$$

Of course, the current is obtained by multiplying Eq. (20) with the normalization constant defined in Eq. (11).

2.5 GENERAL-ELECTRON-CURRENT FUNCTION FOR RETARDING POTENTIAL

This section contains the derivation of the general-electron-current function for the case in which the electrons in the sheath encounter a retarding potential.

In Eq. (8) the lower limit of the radial velocity component u_x of the ion was zero for the accelerating collector potential. When an electron enters the sheath and experiences a retarding potential, then the least radial velocity component, u_1, necessary for its collection is $\sqrt{2eV/m}$. Hence, in integrating the right-hand side of Eq. (8) the lower limit of $u_x = u_1 = \sqrt{2eV/m}$ must be used. Also, in the trajectory relation (3), care must be exercised in selecting the proper sign of eV; in this case the sign is clearly positive since both e and V are negative.

The integral expression for the general-electron current, I_e, is, therefore, given by

$$\text{Lae} \int_0^{2\pi} \int_{u_1}^{\infty} \int_{-\infty}^{\infty} \int_{-p_1}^{p_1} u_x \, F(u_x,u_y,u_z,\beta)\, du_x du_y du_z \, d\beta \qquad (21)$$

where the symbols have their usual meaning.

The solution of Eq. (21) is discussed in Appendix C. The final result in the normalized form is given below,

$$I_{ne} = \exp[-(\overline{V}+\kappa^2)] \sum_{n=0}^{\infty} \frac{(2n+1)!}{(n!)^2 2^{2k}} (\kappa/\sqrt{\overline{V}})^n \, I_n(2\kappa\sqrt{\overline{V}}) \qquad (22)$$

where $I_n(x)$ is the modified Bessel function of the first kind and nth order. The series converges very rapidly for small values of κ; for instance, when $\kappa = 0.3$, the first three terms of the series gives the result correct to

within four parts in ten thousand. Equation (22) was also derived by Mott-Smith and Langmuir,[4] except that their result was for the case of orientation angle $\theta = 90°$.

Since Eq. (22) is derived for the case in which the collector potential, V, is negative, the probe velocity, which never even begins to approach the most probable velocity of the electrons, can always be ignored. Consequently, for $\kappa = 0$, Eq. (22) reduces to

$$I_{ne}\Big|_{\kappa\to 0} = e^{-\mathcal{V}} \tag{23}$$

When the ion current to the collector which is at positive potential with respect to the plasma is considered, for $\lambda \geq 1$, Eq. (22) must be used. Equation (23) for the retarded ion current holds only when $\lambda = 0$ or $\theta = 0$.

2.5.1 Random-Electron-Current Function

When $\mathcal{V}$ is negligibly small, in other words, when the collection of electrons is random, it can be shown that Eqs. (21) and (22) reduce to

$$I_{nr} = e^{-\kappa^2}\left[(1+\kappa^2)I_0(\kappa^2/2) + \kappa^2 I_1(\kappa^2/2)\right] \tag{24}$$

where I_{nr} represents the normalized random electron current.

For $\kappa \cong 0$, which is always true in the case of electrons, Eq. (24) becomes

$$I_{nr}\Big|_{\kappa\to 0} = 1 \tag{25}$$

Comparison of Eq. (24) with the sheath-area-limited ion current function (19) shows that the two cases differ functionally from each other only by the

factor (a/r).

In Section 3 we will use the current functions in predicting the volt-ampere characteristics of the cylindrical probe.

3. DISCUSSION

Since in practice Langmuir probe characteristics are usually interpreted in the voltage range which is negative with respect to the plasma, the current characteristics will be presented for this range only. In other words we need consider only the accelerated ion and the retarded electron currents.

A close examination of Eq. (12) for the accelerated general-ion current shows that the equation contains two parameters, γ_o and $\overline{V}$, which are not independent of each other. Since by definition $\gamma_o = \sqrt{r^2/(a^2-r^2)}$ and $\overline{V} = eV/kT$, an independent relation between (a/r) and V to solve for one of these two parameters is needed in conjunction with Eq. (12) to obtain the actual ion current characteristics.

3.1 ORBITAL-MOTION-LIMITED CURRENT CHARACTERISTICS

Since the orbital-motion-limited current, Eq. (15a) or Eq. (15b), is independent of (a/r), we do not need an independent relation, as we need for the general case, to solve for a/r as a function of V.

In order to obtain the ion current characteristics for a given collector radius and ion density, we first multiply Eq. (15b) with the normalization constant given in Eq. (11). Thus

$$I_o = \sqrt{\frac{kT}{2m\pi}}\ NeA_c\ I_{no} \tag{26}$$

where I_o represents the orbital-motion-limited current and I_{no} is given by Eq. (15a) or (15b). Since the right-hand side of Eq. (26) is a function of

the probe velocity λ and of the orientation angle θ, we fix λ and parameterize θ. Figure 3 illustrates the normalized ion current drawn versus $\bar{V}$ for $\lambda = 1$ and $\theta = 0, 45°, 90°$. The curve for $\theta = 0°$ also describes the stationary probe characteristic, i.e., $\lambda = 0$. This, of course, follows from the fact that $(\kappa = \lambda \sin \theta) = 0$ when either $\lambda = 0$ or $\theta = 0$. Similarly in Figs. 4 and 5, which are drawn for $\lambda = 2$ and $\lambda = 3$ respectively, both $\theta = 0$ curves correspond to the stationary probe case. As one would expect, and as is demonstrated in Figs. 4 and 5, the orientation effect is relatively pronounced at higher probe velocities.

Figure 6 illustrates the stationary probe characteristic, $\lambda = 0$, in which the net current is drawn versus the applied difference of potential δV between the collector and the reference, for $T = 1600°K$ and $N = 10^5$ particles/cc. Of course for $\lambda = 0$, no orientation effect is involved. Figure 7 is drawn for $\lambda = 1$ and the range of θ as shown. Here, as one would expect, the orientation effect is visible mostly in the positive ion current region. Figure 8 demonstrates the similar behavior at $\lambda = 2$, where the orientation effect is even more pronounced.

Thus, in reducing the ion density from experimental data, it is evident from Figs. 7 and 8 that the effects of orientation must be considered. For instance, we must know the measured current, probe velocity, θ, V, and assumed values of T and ion mass to determine the ion density from Eq. (26).

Figure 9 illustrates the electron current characteristic for $\lambda = 2$ and for all θ. Since the net ion current component for all θ is small compared with the electron current component, the orientation angle has a negligible

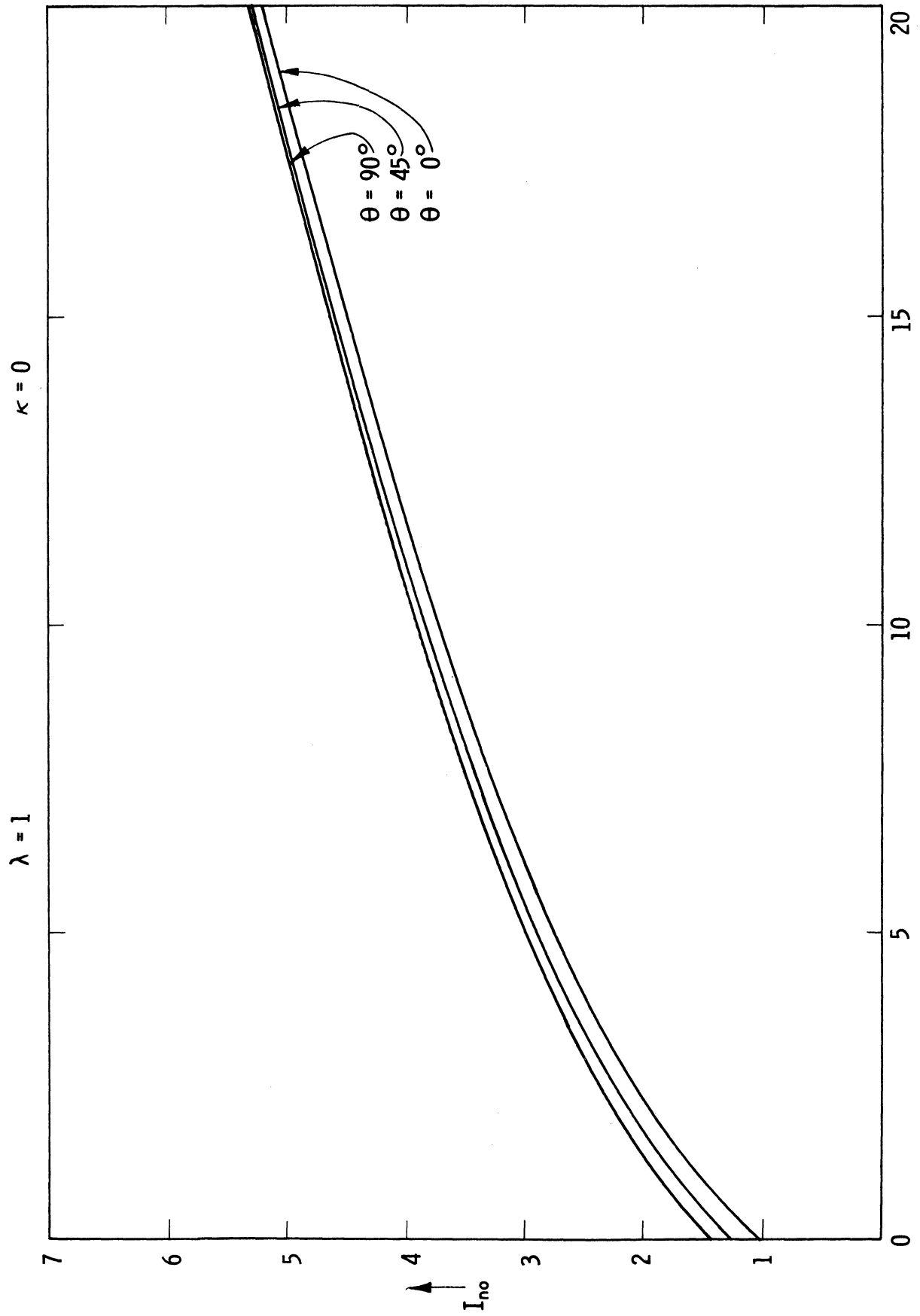

Fig. 3. Normalized orbital-motion-limited ion current I_{no} vs. V, $\lambda = 1$, $\theta = 0$, 45°, 90°.

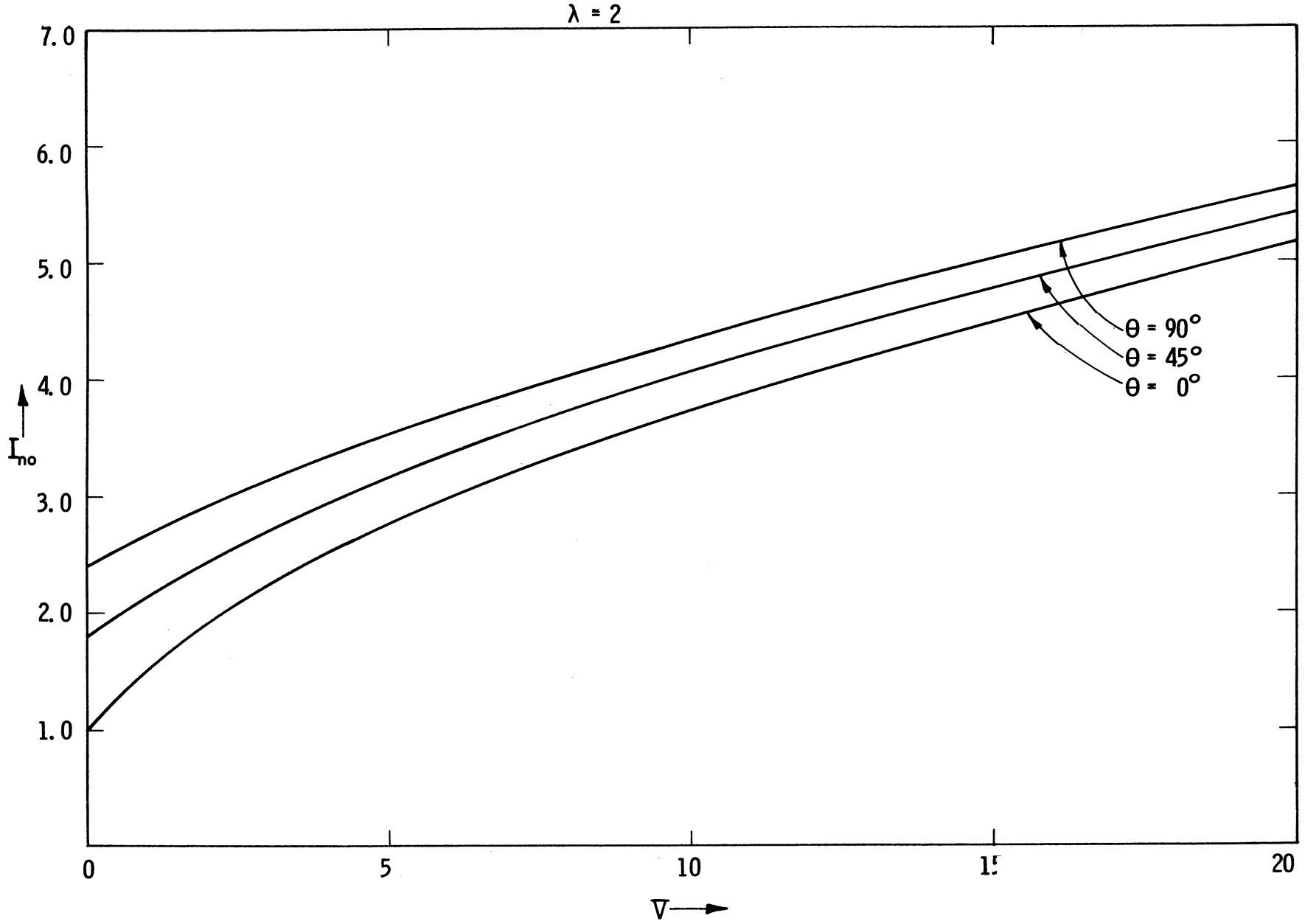

Fig. 4. Normalized orbital-motion-limited ion current I_{no} vs. V, $\lambda = 2$, $\theta = 0, 45°, 90$.

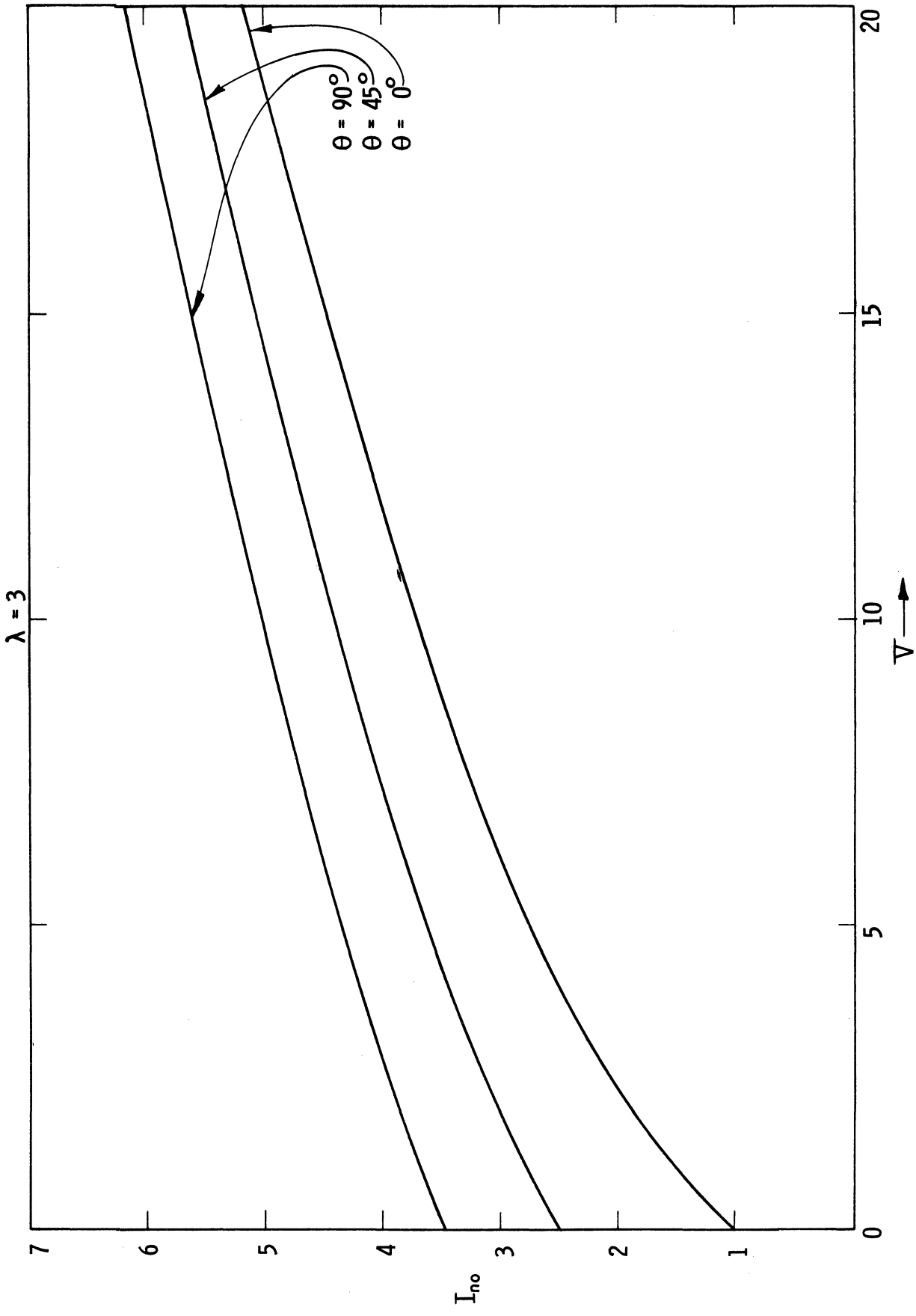

Fig. 5. Normalized orbital-motion-limited ion current I_{no} vs. V, $\lambda = 3$, $\theta = 0$, 45°, 90°.

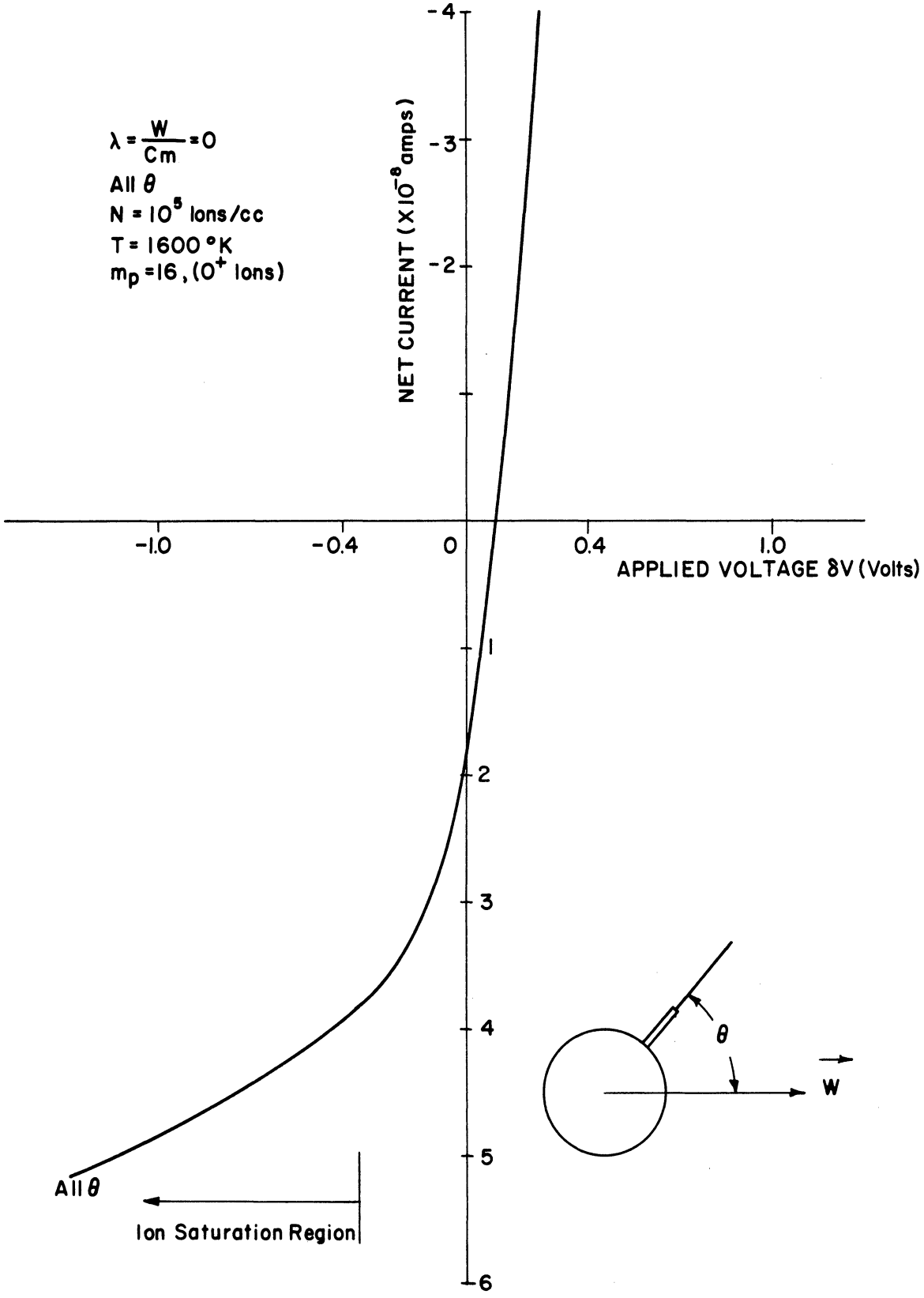

Fig. 6. A predicted volt-ampere characteristic of a stationary thin cylindrical Langmuir probe, under typical F_1 region conditions, showing primarily the ion saturation region of the current characteristic.

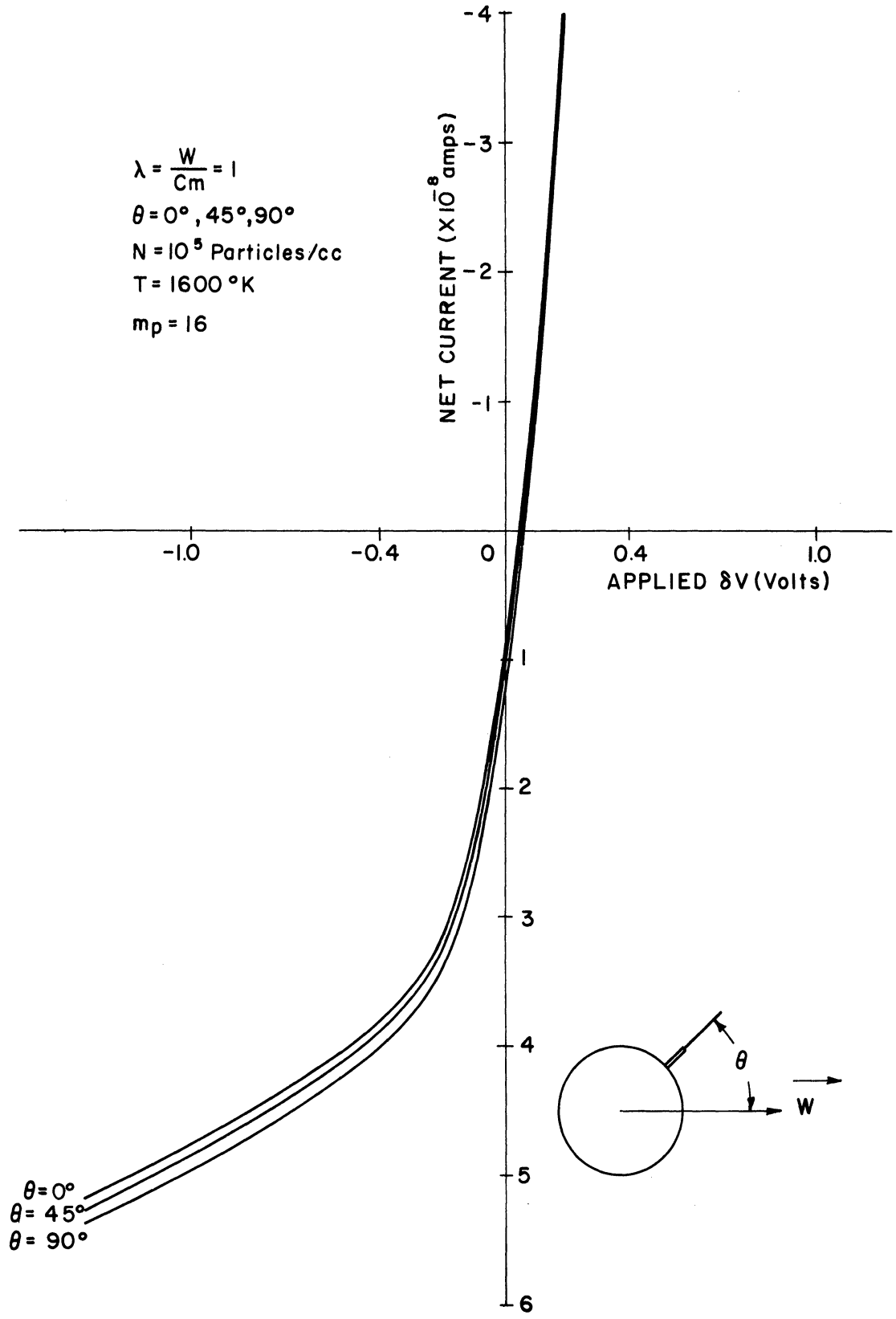

Fig. 7. A predicted volt-ampere characteristic of a cylindrical probe illustrating the effect of orientation upon the ion current characteristic at a fixed velocity ratio, $\lambda = 1$.

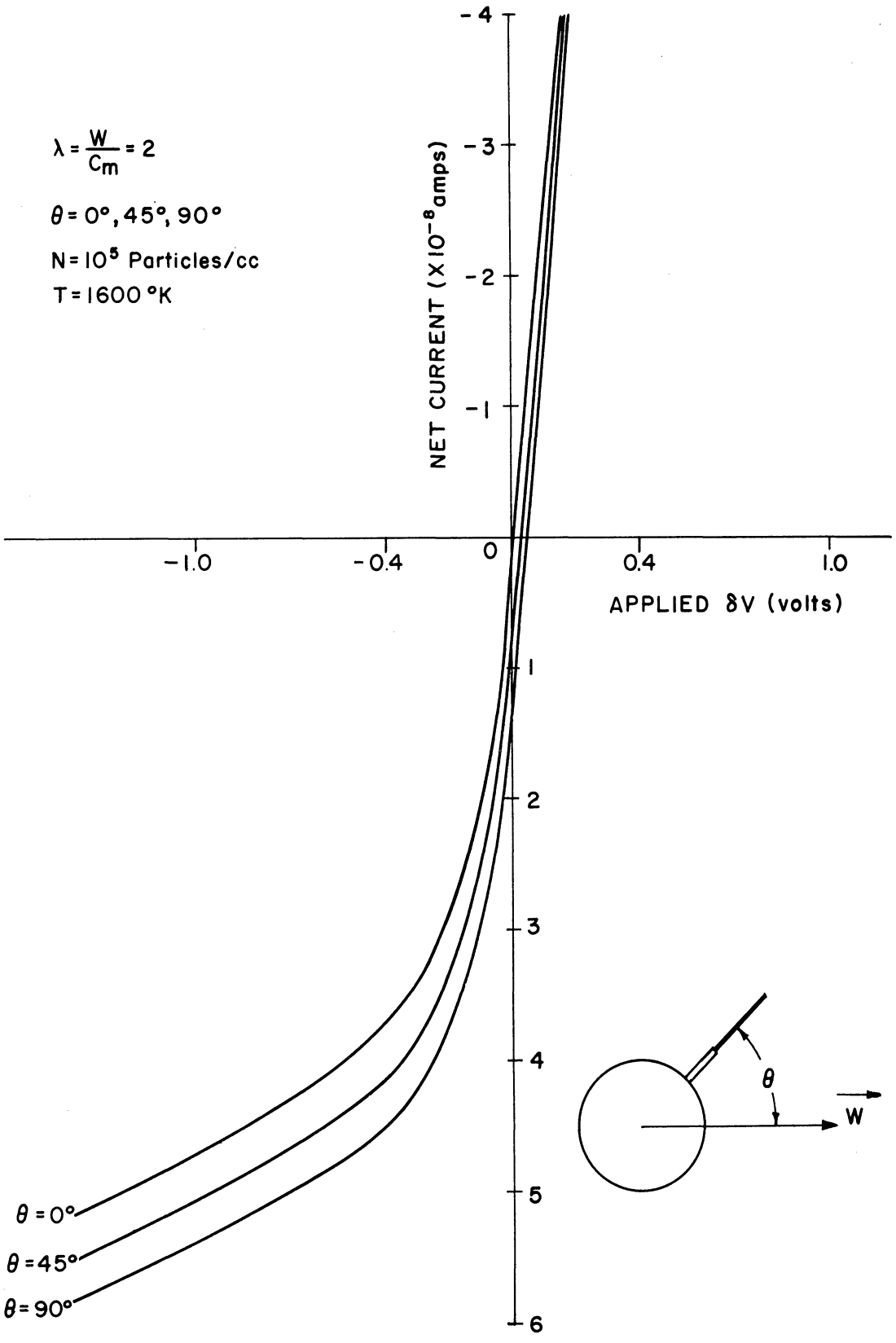

Fig. 8. A predicted volt-ampere characteristic of a cylindrical probe illustrating the effect of orientation upon the ion current characteristic at a fixed velocity ratio, $\lambda = 2$.

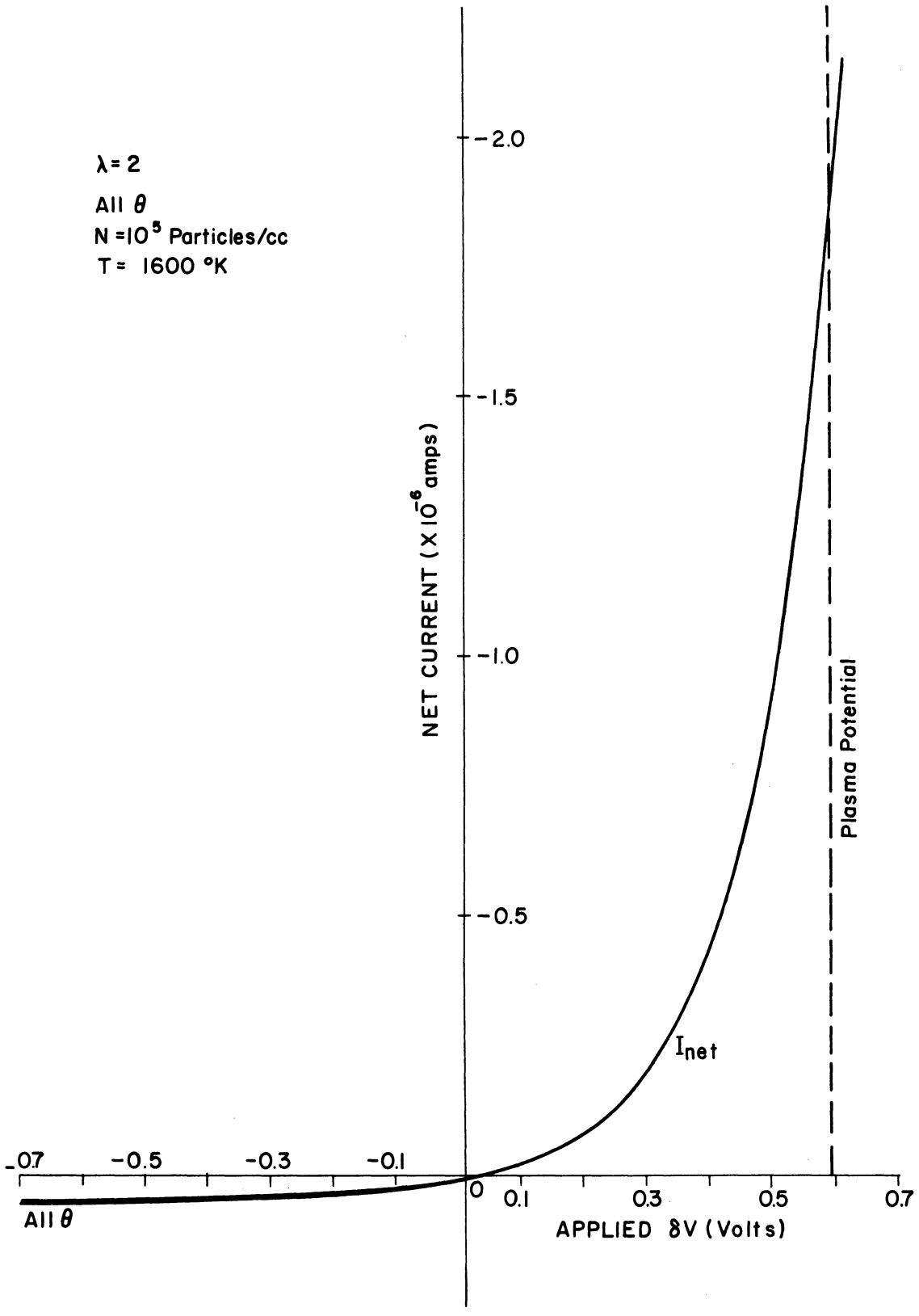

Fig. 9. A predicted volt-ampere characteristic of a cylindrical probe showing primarily the electron current region of the curve from which the electron temperature may be derived.

effect on determination of the electron temperature. Thus with the help of Eq. (23) we can determine the electron temperature by plotting the natural logarithm of the electron current versus the applied voltage. Rearrangement of Eq. (23) for the electron temperature yields Eq. (27):

$$T_e = -e/k \frac{d}{d\delta V} (\log_e I_e|_{\kappa \to 0}) \tag{27}$$

where subscript e refers to the electron parameters.

3.2 SHEATH-AREA-LIMITED CURRENT CHARACTERISTICS

For the extreme case in which all the ions that enter the sheath reach the collector, the current function given by Eq. (19) is dependent on (a/r) and κ only. For this reason we do not need an independent relation to solve for the current, as we do in the case of the general-ion-current function (12).

In Fig. 10, which illustrates the functional behavior of Eq. (19), $f(\kappa)$ is drawn versus λ with θ parameterized. Since $f(\kappa)$ alone represents the random-current function, Fig. 10 is also representative of the random-electron-current function, which is inherently independent of "a." For electrons, however, λ is nearly zero even for the satellite velocities; hence the curve for $\theta = 0$ in Fig. 10 represents the relevant electron-current characteristic. Functionally the behavior of the random-electron-current function is exactly the same as that of the sheath-area-limited ion current function.

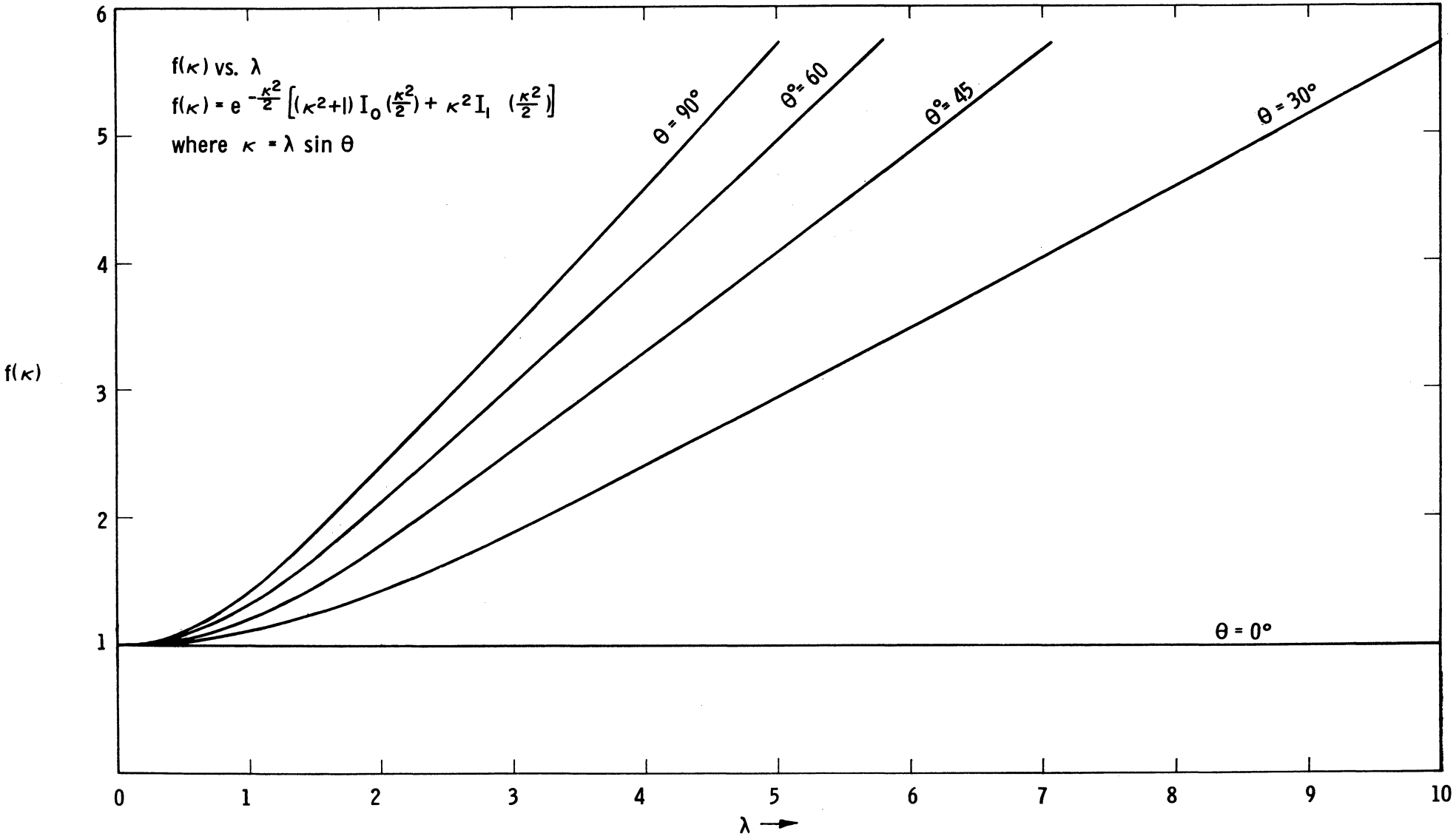

Fig. 10. Random current function drawn versus the velocity ratio illustrating the orientation effect.

APPENDIX A

POLAR TRANSFORMATION OF THE GENERAL-ION-CURRENT FUNCTION FOR ACCELERATING POTENTIAL (-V)

It can be shown by plotting u_x, p_1 as rectangular coordinates of a point that Eq. (3), when V is negative and e is positive, reads:

$$p_1^2 = \frac{r^2}{a^2-r^2}\left(u_x^2 + \frac{2eV}{m}\right)$$

This equation is a hyperbola whose semi-axes are

$$\left(\frac{2eV}{m}\right)^{1/2} \Big/ \left(\frac{a^2}{r^2} - 1\right), \quad i\left(\frac{2eV}{m}\right)^{1/2}$$

on the p_1 and u_x axes respectively. Since integral (8) is an even function of u_z, it is sufficient to show only one branch of the hyperbola. This is illustrated in Fig. 11 where $\gamma_o = \sqrt{r^2/(a^2-r^2)}$. After integrating Eq. (8) for β and u_y, we have

$$I = \frac{4LNae}{C_m^2} e^{-\kappa^2} \int_0^\infty \int_0^{p_1} u_x \exp\left[-\frac{1}{C_m^2}\left(u_x^2 + u_z^2\right)\right] I_o\left[2\kappa\sqrt{\frac{1}{C_m^2}\left(u_x^2+u_z^2\right)}\right] du_x du_z \qquad \text{(A-1)}$$

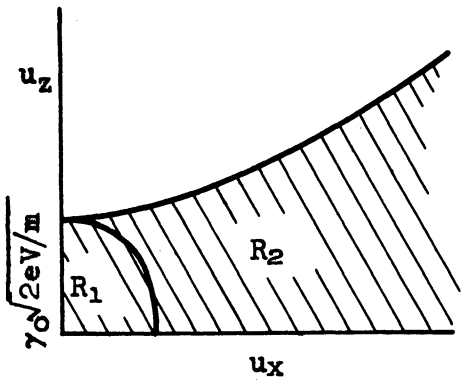

Fig. 11. Hyperbola generated in velocity-space coordinate system by p_1 as a function of u_x.

and the domain of integration is the one enclosed by the hyperbola shown shaded in Fig. 11. Let

$$\begin{aligned} u_x/C_m &= s \cos \psi \\ u_z/C_m &= p_1/C_m = s \sin \psi \\ du_x du_z &= C_m^2 \, s \, ds \, d\psi \end{aligned} \tag{A-2}$$

Now divide both sides of Eq. (3) with C_m^2, obtaining

$$\frac{p_1^2}{C_m^2} = \gamma_o^2 \left(\frac{u_x^2}{C_m^2} + \overline{V}\right) \tag{A-3}$$

where $\overline{V} = 2eV/mC_m^2 = eV/kT$, the normalized voltage (not to be confused with the normalized current).

Substitute Eq. (A-2) in Eq. (A-3) to obtain

$$\psi_1 = \sin^{-1} \sqrt{\gamma_o^2(s^2+V)/s^2(1+\gamma_o^2)} \tag{A-4}$$

This means that if we divide the hyperbolic domain shown in Fig. 11 into two regions, R_1 and R_2, then Eq. (A-4) yields the ψ variance in region R_2 with respect to the hyperbola. Thus the limits of integration of Eq. (A-1) in region R_2 are

$$\begin{aligned} 0 \le \psi \le \psi_1 \\ \gamma_o \sqrt{\overline{V}} \le s < \infty \end{aligned} \tag{A-5}$$

and in region R_1 the limits are

$$\begin{aligned} 0 \le \psi \le \pi/2 \\ 0 \le s \le \gamma_o \sqrt{\overline{V}} \end{aligned} \tag{A-6}$$

Insert the polar transformation of the coordinates given in Eqs. (A-2) and the limits of integration given by Eqs. (A-5) and (A-6) in Eq. (A-1) to obtain

$$I = 4LNae\, C_m\, e^{-\kappa^2}\left[\iint_{R_2} s^2\cos\psi\; e^{-s^2} I_o(2\kappa s)\,ds\,d\psi + \iint_{R_1} s^2\cos\psi\; e^{-s^2} I_o(2\kappa s)\,ds\,d\psi\right]$$

which, on integrating with respect to ψ and rearranging the terms, becomes

$$I = \sqrt{\frac{kT}{2m\pi}}\, NeA_c\, \frac{4}{\sqrt{\pi}}\, e^{-\kappa^2}\left[\int_{\gamma_o\sqrt{V}}^{\infty} s(s^2+V)^{1/2}\, e^{-s^2}\, I_o(2\kappa s)\,ds + \sqrt{\frac{1+\gamma_o^2}{\gamma_o^2}}\int_o^{\gamma_o\sqrt{V}} s^2\, e^{-s^2}\, I_o(2\kappa s)\,ds\right] \qquad \text{(A-7)}$$

This corresponds to Eq. (9) given in Section 2.4.

APPENDIX B

STEPS INVOLVED IN ARRIVING AT THE SOLUTION OF THE GENERAL-ION-CURRENT FUNCTION

There are two integrals given in Eq. (9) which we desire to solve. In the first integral

$$I_1 = \int_{\gamma_o\sqrt{V}}^{\infty} s(s^2+V)^{1/2}\, e^{-s^2}\, I_o(2\kappa s)\, ds \qquad \text{(B-1)}$$

Put

$$s^2 + V = t$$

$$sds = \frac{dt}{2}$$

to obtain

$$I_1 = \frac{1}{2} e^{V} \int_{V(1+\gamma_o^2)}^{\infty} t^{1/2}\, e^{-t}\, I_o(2\kappa\sqrt{t-V})\, dt \qquad \text{(B-2)}$$

and expand the Bessel function. Thus

$$I_1 = \frac{1}{2} e^{V} \sum_{k=0}^{\infty} \frac{\kappa^{2k}}{(k!)^2} \int_{V(1+\gamma_o^2)}^{\infty} t^{1/2}(t-V)^k\, e^{-t}\, dt \qquad \text{(B-3)}$$

Binomial expansion of the term $(t-V)^k$ in the integrand of (B-3) yields

$$I_1 = \frac{1}{2} e^{V} \sum_{k=0}^{\infty} \sum_{n=0}^{k} \frac{\kappa^{2k}(-V)^{k-n}}{k!(k-n)!n!} \int_{V(1+\gamma_o^2)}^{\infty} t^{n+1/2}\, e^{-t}\, dt \qquad \text{(B-4)}$$

Now according to the definitions of the incomplete gamma functions[7]

$$\gamma(\nu,x) = \int_o^x e^{-t}\, t^{\nu-1}\, dt \qquad \text{(B-5)}$$

$$\Gamma(\nu,x) = \int_x^{\infty} e^{-t}\, t^{\nu-1}\, dt \qquad \text{(B-6)}$$

the right-hand side of Eq. (B-4) may be written as

$$I_1 = \frac{1}{2} e^{\nabla} \sum_{k=0}^{\infty} \sum_{n=0}^{k} \frac{\kappa^{2k}(-\nabla)^{k-n}}{k!(k-n)!n!} \Gamma [n + \frac{3}{2}, \nabla(1+\gamma_o^2)] \qquad \text{(B-7)}$$

In Eq. (B-7) use the following lemma:[8]

$$\sum_{k=0}^{\infty} \sum_{n=0}^{k} A(k,n) = \sum_{k,n=0}^{\infty} A(k+n,n) \qquad \text{(B-8)}$$

Thus we obtain

$$I_1 = \frac{1}{2} e^{\nabla} \sum_{k,n=0}^{\infty} \frac{\kappa^{2k+2n}(-\nabla)^{k}}{(k+n)!k!n!} \Gamma [n + \frac{3}{2}, \nabla(1+\gamma_o^2)] \qquad \text{(B-9)}$$

Since the Bessel function of order n is defined as

$$J_n(z) = \sum_{k=0}^{\infty} \frac{(-1)^k (z/2)^{2k+n}}{k!(n+k)!}$$

Then Eq. (B-9) after summing with respect to k may be written as

$$I_1 = \frac{1}{2} e^{\nabla} \sum_{n=0}^{\infty} \frac{(\kappa/\sqrt{\nabla})^n}{n!} \Gamma [n + \frac{3}{2}, \nabla(1+\gamma_o^2)] J_n(2\kappa\sqrt{\nabla}) \qquad \text{(B-10)}$$

Hence Eq. (B-10) is the solution of integral (B-1), the first integral of Eq. (9). Similarly, the second integral of Eq. (9) may be solved as follows:

$$\begin{aligned} I_2 &= \int_0^{\gamma_o\sqrt{\nabla}} s^2 e^{-s^2} I_0(2\kappa s) ds \\ &= \sum_{n=0}^{\infty} \frac{\kappa^{2n}}{(n!)^2} \int_0^{\gamma_o\sqrt{\nabla}} s^{2n+2} e^{-s^2} ds \\ &= \frac{1}{2} \sum_{n=0}^{\infty} \frac{\kappa^{2n}}{(n!)^2} \int_0^{\gamma_o^2\nabla} t^{n+1/2} e^{-t} dt \end{aligned}$$

Using the definition (B-5) of the incomplete gamma function we obtain

$$I_2 = \frac{1}{2} \sum_{n=0}^{\infty} \frac{\kappa^{2n}}{(n!)^2} \gamma\left(n + \frac{3}{2}, \gamma_o^2 V\right) \qquad \text{(B-11)}$$

Thus Eq. (B-11) provides the solution for the second integral of Eq. (9).

APPENDIX C

SOLUTION OF THE ORBITAL-MOTION-LIMITED ION CURRENT INTEGRAL

The required integral to be solved is Eq. (14), which is given by

$$I = \int_0^\infty s(s^2+V)^{1/2} e^{-s^2} I_0(2\kappa s)\,ds \qquad (C\text{-}1)$$

where we have omitted the factor $\exp(-\kappa^2)4/\sqrt{\pi}$.

There are various ways of solving Eq. (C-1). We will choose two methods which provide the solutions in power series; one of the two can be computed easily. But before proceeding further, it would be expedient to define what is called a "confluent hypergeometric function."

Any solution of Kummer's confluent hypergeometric differential equation, given as Eq. (C-2), is called a "confluent hypergeometric function."[9]

$$x\frac{d^2y}{dx^2} + (b-x)\frac{dy}{dx} - ay = 0 \qquad (C\text{-}2)$$

The simplest solution of Eq. (C-2) is Kummer's hypergeometric function:

$${}_1F_1(a;b;x) = 1 + \frac{a}{b}x + \frac{a(a+1)}{b(b+1)}\frac{x^2}{2!} + \frac{a(a+1)(a+2)}{b(b+1)(b+2)}\frac{x^3}{3!} + \cdots \qquad (C\text{-}3)$$

There are several notations in use for series (C-3). In this work it will be denoted by

$${}_1F_1(a;b;x) = \sum_{n=0}^{\infty} \frac{(a)_n}{(b)_n}\frac{x^n}{n!} \qquad (C\text{-}4)$$

where $(a)_n$ and $(b)_n$ are the "factorial functions" defined as

$$(a)_n = \frac{\Gamma(a+n)}{\Gamma(a)}$$

$$= \prod_{j=1}^{n} (a+j-1)$$

$$= a(a+1)(a+2) \cdots (a+n-1) \qquad (C\text{-}5)$$

It is clear from the definition (C-5) that the factorial function is the generalized form of the gamma function.

The integral representation of the confluent hypergeometric function (C-4) is

$${}_1F_1(a;b;x) = \frac{\Gamma(b)}{\Gamma(a)\,\Gamma(b-a)} \int_0^1 e^{xt}\, t^{a-1}(1-t)^{b-a-1}\, dt \qquad (C\text{-}6)$$

in which $\mathrm{Re}(b) > \mathrm{Re}(a) > 0$.

In the process of integrating Eq. (C-1) we will also use the following lemma,[8]

$$\sum_{n=0}^{\infty} \sum_{k=0}^{n} B(k,n) = \sum_{n=0}^{\infty} \sum_{k=0}^{\infty} B(k,n+k) \qquad (C\text{-}7)$$

and Lengendre's duplication formula[8]

$$\sqrt{\pi}\,\Gamma(2z) = 2^{2z-1}\,\Gamma(z)\,\Gamma\left(z+\tfrac{1}{2}\right) \qquad (C\text{-}8)$$

With this background we can proceed toward the solution of Eq. (C-1), in which we substitute $s^2+V = Vy$ to obtain

$$I = \frac{V^{3/2}}{2}\, e^{V} \int_1^{\infty} y^{1/2}\, e^{-Vy}\, I_0\left(2\kappa V^{1/2}\sqrt{y-1}\right) dy$$

Now expand the modified Bessel function and break the integral into two parts.

Thus

$$I = \frac{V^{3/2}}{2} e^{V} \sum_{n=0}^{\infty} \frac{(-1)^n (\kappa\sqrt{V})^{2n}}{(n!)^2} \left[\int_0^{\infty} y^{1/2}(1-y)^n e^{-Vy} dy - \int_0^{1} y^{1/2}(1-y)^n e^{-Vy} dy \right] \tag{C-9}$$

Take each integral in (C-9) separately:

$$\int_0^{\infty} y^{1/2}(1-y)^n e^{-Vy} dy = \sum_{k=0}^{n} \frac{(-1)^k n!}{(n-k)!k!} \int_0^{\infty} y^{k+1/2} e^{-Vy} dy$$

$$= \sum_{k=0}^{n} \frac{(-1)^k n!}{(n-k)!k!} \frac{\Gamma(k+3/2)}{V^{k+3/2}} \tag{C-9a}$$

From the integral representation of the confluent hypergeometric function as given by Eq. (C-6) we obtain the solution for the second integral in Eq. (C-9), in which a = 3/2, b = n+5/2, and z = -V. Thus

$$\int_0^{1} y^{1/2}(1-y)^n e^{-Vy} dy = \frac{\Gamma(3/2)\Gamma(n+1)}{\Gamma(n+5/2)} {}_1F_1(3/2;n+5/2;-V) \tag{C-9b}$$

Substitute (C-9a) and (C-9b) in Eq. (C-9) to obtain

$$I = \frac{V^{3/2}}{2} e^{V} \sum_{n=0}^{\infty} \frac{(-1)^n (\kappa\sqrt{V})^{2n}}{(n!)^2} \left[\sum_{k=0}^{n} \frac{(-1)^k n!}{(n-k)!k!} \frac{\Gamma(k+3/2)}{V^{k+3/2}} - \frac{\Gamma(3/2)\Gamma(n+1)}{\Gamma(n+5/2)} {}_1F_1(3/2;n+5/2;-V) \right]$$

$$I = \frac{V^{3/2}}{2} e^{V} \left[\sum_{n=0}^{\infty} \sum_{k=0}^{n} \frac{(-1)^{n+k} \Gamma(k+3/2)(\kappa\sqrt{V})^{2n}}{n!(n-k)!k!V^{k+3/2}} - \Gamma(3/2) \sum_{n=0}^{\infty} \frac{(-1)^n (\kappa\sqrt{V})^{2n} {}_1F_1(3/2;n+5/2);-V)}{n!\Gamma(n+5/2)} \right] \tag{C-10}$$

In Eq. (C-10) use Lemma (C-7) in the first part and expand the hypergeometric function in the second part according to the definition (C-4), obtaining

$$I = \frac{\nabla^{3/2}}{2} e^{\nabla} \left[\sum_{n,k=0}^{\infty} \frac{(-1)^n (\kappa\sqrt{\nabla})^{2n}}{n!(n+k)!} \frac{\Gamma(k+3/2)\kappa^k}{k!(\sqrt{\nabla})^{k+3}} \right.$$

$$\left. - \sum_{n,k=0}^{\infty} \frac{(-1)^n (\kappa\sqrt{\nabla})^{2n+k+3/2}}{n!\Gamma(n+k+5/2)} \frac{(-1)^k \Gamma(k+3/2)(\sqrt{\nabla})^k}{k!\kappa^{k+3/2}\nabla^{3/4}} \right] \tag{C-11}$$

Now according to the definitions of the cylindrical and the spherical Bessel functions, we have

$$J_k(2z) = \sum_{n=0}^{\infty} \frac{(-1)^n (z)^{2n+k}}{n!(n+k)!} \tag{C-11a}$$

$$J_{k+3/2}(2z) = \sum_{n=0}^{\infty} \frac{(-1)^n (z)^{2n+k+3/2}}{n!\Gamma(n+k+5/2)} \tag{C-11b}$$

Using (C-11a) and (C-11b) in Eq. (C-11) we obtain

$$I = \frac{1}{2} e^{\nabla} \left[\sum_{k=0}^{\infty} \frac{\Gamma(k+3/2)}{k!} (\kappa/\sqrt{\nabla})^k J_k(2\kappa\sqrt{\nabla}) \right.$$

$$\left. - \sum_{k=0}^{\infty} \frac{(-1)^k \Gamma(k+3/2)}{k!} (\sqrt{\nabla}/\kappa)^{k+3/2} J_{k+3/2}(2\kappa\sqrt{\nabla}) \right] \tag{C-12}$$

From Legendre's duplication formula, (C-8), we obtain

$$\Gamma(k+3/2) = \frac{\sqrt{\pi}\,\Gamma(2k+2)}{2^{2k+1}\Gamma(k+1)} = \frac{\sqrt{\pi}\,(2k+1)!}{2^{2k+1}\,k!}$$

Hence

$$I = \frac{\sqrt{\pi}}{4} e^{\nabla} \sum_{k=0}^{\infty} \frac{(2k+1)!}{2^{2k}(k!)^2} \left[(\kappa/\sqrt{\nabla})^k J_k(2\kappa\sqrt{\nabla}) \right.$$

$$\left. - (-1)^k (\sqrt{\nabla}/\kappa)^{k+3/2} J_{k+3/2}(2\kappa\sqrt{\nabla}) \right] \qquad \text{(C-13)}$$

Multiplication of Eq. (C-13) with the factor $\exp(-\kappa^2) 4/\sqrt{\pi}$ yields the right-hand side of Eq. (15a).

The steps involved in obtaining the second solution of Eq. (14), given by Eq. (15b), are shown in Appendix B.

ACKNOWLEDGMENTS

The author wishes to express his deep gratitude to the following individuals: Andrew F. Nagy for making many useful suggestions in the preparation of this report; particularly Walter Hoegy for reading and helping to organize the report; Hugo DiGiulio for programming the current equations; Salma Khammash for plotting the graphs; Rosann Burke, secretary of the project, for typing the manuscript; and George Carignan and L. H. Brace, present and past directors of the project, for many useful discussions.

REFERENCES

1. Boggess, R. L., Electrostatic Probe Measurements of the Ionosphere, Univ. of Mich. ORA Report No. 2521, 2816-1, 03484-1-S, Ann Arbor, Nov. 1959.

2. Hoegy, W. R., and Brace, L. H., The Dumbbell Electrostatic Ionosphere Probe: Theoretical Aspects, Univ. of Mich. ORA Report No. 03599-5-S, Ann Arbor, Sept. 1961.

3. Kanal, M., Brace, L. H., and Caldwell, J. R., An Ejectable Ion Trap-Langmuir Probe Experiment for Ionosphere Direct Measurements, Univ. of Mich. ORA Report No. 03484-3-S, Ann Arbor, July 1962.

4. Mott-Smith, H. M., and Langmuir, I., "Theory of Collectors in Gaseous Discharges," Phys. Rev. 28 (Oct. 1926).

5. Kanal, M., Theory of Current Collection of Moving Spherical Probes, Univ. of Mich. ORA Report No. 03599-9-S, Ann Arbor, April 1962.

6. Langmuir, I., "Electrical Discharges in Gases," Part II, Rev. Mod. Phys. 3 (April 1931).

7. Bateman Manuscript Project, Higher Transcendental Functions, Vol. 2, McGraw-Hill Book Co., 1953.

8. Rainville, E. D. (Univ. of Mich.), Special Functions, Macmillan, 1960.

9. Slater, L. J., Confluent Hypergeometric Functions, Cambridge Univ. Press, 1960.

See also:

Magnus, W., and Oberhettinger, F., Functions of Mathematical Physics, Chelsea, 1954.